WILEY | Hindawi

Research Article

Optimization Drive on a Flat Tire Vehicular System for Autonomous E-Vehicles Using Network Distribution Simulations

V Sivamaran,[1] **Hariprasath Manoharan** ⓘ**,**[2] **Yuvaraja Teekaraman** ⓘ**,**[3]
Ramya Kuppusamy,[4] **and Arun Radhakrishnan** ⓘ[5]

[1]*Department of Mechanical Engineering, Audisankara College of Engineering and Technology, Andhra Pradesh 524 101, India*
[2]*Department of Electronics and Communication Engineering, Panimalar Institute of Technology, Tamil Nadu 600 123, India*
[3]*Department of Electronic and Electrical Engineering, The University of Sheffield, Sheffield, S1 3JD, UK*
[4]*Department of Electrical and Electronics Engineering, Sri Sairam College of Engineering, Bangalore 562106, India*
[5]*Faculty of Electrical and Computer Engineering, Jimma Institute of Technology, Jimma University, Jimma, Ethiopia*

Correspondence should be addressed to Yuvaraja Teekaraman; y.teekaraman@sheffield.ac.uk and Arun Radhakrishnan; arun.radhakriahnan@ju.edu.et

The run-on flat tire is an important technology in the area of vehicle safety technology. Nowadays, traveling by a personal vehicle from one place to another has increased due to the increase in the global economy. The main problem that is faced while traveling is tire puncture. The tire may get punctured by any sharp objects on the road such as screws and iron pins that traps the tire surface. A situation like this may be overcome by the usage of the drive on a puncher tire device which will be used to reach the destination without any need for a puncher shop. Using this device will reduce the damage of the tire and tube. This device is portable and can be placed in a vehicle itself. For this reason, a design has been developed by the CATIA 3D experience. The drive on a puncher tire device was designed using the software developed by the Dassault systems named CATIA 3D experience. Aluminum alloy was chosen as the base material to design and simulate this product. Also, the network distribution simulations were used to develop the mathematical equations to check the adequacy of the model. This device is very useful while traveling long distances if any puncher will occur. The sensors were attached to the product to receive the signal from the vehicle, so that the vehicle will run smoothly for a short distance. Drive on a puncher tire will be suitable for both two- and four-wheeler vehicles and also useful for all the areas like villages, towns, panchayats, and cities. If the tire is puncher, we cannot drive the vehicle; hence, a skating device is fixed at a tired bottom, which is used to move the vehicle. The proposal will be beneficial for a huge number of people who own two and four wheelers. This design and simulation will address the problem of the two- and four-wheeler owners traveling long distances.

1. Introduction

The safety of the automobile vehicles was highly affected by the tire performance. The vehicle accidents caused by punctures are more than 70% [1]. The accidents occurred by the tire puncture cost more than the amount to replace the new tire as well as the damage to the road environment. The most significant reason for the tire puncture is caused by the sharp objects on-road and off-road. These sharp objects make tires to let the air out which tends to sudden failure of the brake system [2–12]. For this purpose, in this investigation, an attempt has been made to design and simulate the roller skater drive system for automobile vehicles to travel a short distance.

The CATIA 3D experience was used to design and simulate the puncture tire drive in an autonomous vehicle. The evolution of the world for the past decade in the field of automobile sector, especially in the design and manufacturing, was mind-blowing. Furthermore, software usage in the automobile industry is developing with new technologies day by day. So, the latest updated version of CATIA V5 software named CATIA 3D experience was used

to design and simulate the drive on a punctured tire. The tire is a rubber product that is used to cover the wheel rim in an automobile vehicle, which acts as a rotating movable body between the vehicle body and the road. The drive on the punctured tire is still underdeveloped. Many new ideas and designs were introduced that allows the tire to run safely without air with limited speed. But none of them were successful at the expected level [13–21]. The skating-like device has three decades of history. Mostly, it was used in the winter season for the snow areas. The skating device is also used for traveling from one place to another on snow roads, mainly in hilly areas. A flat tire may occur in any scenario like tire bubbles, hydroplaning, or aged tires. Even in some tire applications, researchers have added carbon nano-materials to enhance the rigidity of the tires [22].

The research done on run-on puncture tires was different compared to the model proposed in this investigation. The run-on puncture tire includes a double inner cavity, a supporting drive on the punctured tire (see Figure 1), a nonpneumatic mechanical wheel, etc. [23–26]. Some limitations arise while using these drives on flat tire devices. The two independent chambers have been linked with a double inner cavity drive on the flat tire. The double inner cavity drive on a flat tire has a boundary to withstand large puncture holes. Past studies in the area of tire-related research focused on mechanical properties and lightweight design of tires [27–29]. For a short drive on a flat tire, in this investigation, an attempt was made to design and simulate the drive on a punctured tire with an electronic control system using CATIA 3D experience.

1.1. Recent Literature.

From the application point of view, many techniques are highly useful in analyzing the exact position of tires where a MEMS accelerometer plays a vital role in this identity process [30]. In this measurement process, a hybrid system model has been integrated with an electrohydraulic drive and this provides a linear mechanism for management development. This type of linear procedure will reduce the cost of implementation as compared to other sensor types since the dynamic range of the monitoring system is lower in the control process. Even in the practical conventional system, the aforementioned linear procedures are applied with a microcontroller-based system, and it is found that several parameters of tire are directly reported to the corresponding vehicle driver for ensuring a safe drive in presence of rotation angles. In addition, a redundancy check is carried out for the MEMS accelerometer, and it is argued that there is no need to remove hydraulic systems from any point of view.

But in the case of system modernization activities, it is necessary to remove the hydraulic system which is considered a major drawback of the system. In case of removal, a force estimation procedure is followed [31] using a machine learning algorithm by incorporating a triaxis accelerometer sensor. This category of force estimation process provides a prediction of the tire using online procedures with high-risk driving conditions. Conversely, an ideal solution is obtained in this case which is treated as an intelligent operating
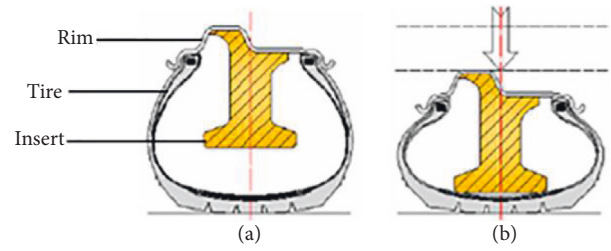

Figure 1: Schematic representation of the ISRFT: (a) normal tire pressure and (b) zero tire pressure.

technique as big data management is processed at the end systems. Both the functions of the abovementioned system with the help of supervised learning technique but to reduce the cost of implementing a system must function effectively with unsupervised learning procedures [32]. As a consequence, a neural network model is introduced with a set of training data which is automatically compared with existing values and reports the changes to the central station. Even three-dimensional data are applied as a training set to prevent the loss of values from the system end. In this way, the conventional technique provides a great insight for capturing the defect that is present in different tires with varying dimensions in Table 1.

1.2. Flat Tire Model: Mathematical Representations.

In this section, a new system model is described for straight tire rolling factors as the position of each point must be defined before the vertical line. This point of interaction can be determined using some selected points that are observed during real-time implementation. Also, a co-ordinate axis representation point with respect to vertical line is also determined by considering the position from a center tire profile. This can be determined by using the Forecast procedure as follows:

$$S_{xi} = \sum_{i=1}^{n} \sin\theta * C_{in}, \qquad (1)$$

where C_{in} denotes the original co-ordinate system that is measured from the center angle.

Equation (1) represents a vertical co-ordinate plane axis with respect to wheel systems, and it is denoted by sine angles. However, it is essential to represent a flat tire system using a horizontal axis which is termed as a reference position that is measured with respect to the cosine angle as denoted in

$$S_{zi} = \sum_{i=1}^{n} \cos\theta * R_{in}, \qquad (2)$$

where R_{in} represents the reference co-ordinate system in the horizontal position of tire pressure.

Equation (2) indicates that the total data radius of tires for all distinct vehicles will be measured and stored as central data for comparison. Thus, minimum and maximum limits are provided with equivalent weight factors that can be represented using Equation (3). At this point of contact, the

TABLE 1: Comparison of the existing and proposed technique.

Reference	Technique	Type of sensor	Type of algorithm
[30]	Linear prediction	MEMS and LVDT sensors	Control algorithm
[31]	Force estimation	Triaxis sensor	Machine learning
[32]	Neural network	Lase sensor	Unsupervised and machine learning
Proposed	CATIA 3D	MEMS accelerometer	Gradient based

weight of the individual tire system is measured with a terrain organization scheme.

$$\gamma_i = \sum_{i=1}^{n} w_i (\sin \theta_i) + w_n (\cos \theta_n), \tag{3}$$

where w_i and w_n indicate the corresponding weight factors at both the co-ordinates and θ_i and θ_n represent equivalent angle positions at both vertical and horizontal axes.

From Equation (3), it can be perceived that two angle representation systems with discrete representation values can be measured with a multiplication factor. The above-mentioned angle of measurement will change if any external force is applied in the system. Thus, changes in representation can be denoted using

$$R_c = \sum_{i=1}^{n} e_{\text{in}} + d_{\text{in}}, \tag{4}$$

where e_{in} and d_{in} indicate reference values with two constituents, namely, flexible and vibrant changes.

In case if more vibrant changes are detected, then a sound alarm will be indicated to the driver to prevent immediate accident and this can be treated as the last state of warning systems. Furthermore, if any rotation is found, then slip path indications will be measured with the rotation factor as given in

$$S_f = \sum_{i=1}^{n} rc_i * fs_{\text{in}}, \tag{5}$$

where rc_i denotes the rotating path curvature of vehicles and fs_{in} represents the forward speed with imaginary point detection.

Conversely, the moving speed of vehicles cannot be measured in an accurate way during the rotation axis; thus, in addition to slip angle, an adjacent slip point is measured that is represented using

$$\vartheta_i = \sum_{i=1}^{n} a_{sp}(i) * \sin(\arctan(x_i)), \tag{6}$$

where $a_{sp}(i)$ represents the adjacent slip point at i^{th} position and $\arctan(x_i)$ denotes the arctan angle with curve shape points.

Any sudden changes in force will be measured with change in latitude and longitude velocities as tires are unloaded where drivers are not alert about changing conditions. Therefore, a deflection rate is calculated with time-changing velocities as indicated in

$$\frac{d(u)}{d(t)} = \sum_{i=1}^{n} (\mu_x - \mu_z), \tag{7}$$

where μ_x and μ_z denote velocity components with cross rebound values.

The obtained values in Equation (7) will be differentiated with time periods that are measured at both vertical and horizontal points. Thus, the sum of values in Equations (3) and (7) provides a low-risk percentage that avoids alert measuring points. The point of integrating the system model with the corresponding algorithm is discussed in subsequent sections.

2. Optimization Algorithms

In this section, a GBA is implemented with a MEMS accelerometer as the position and velocity of wheels varied with changing time periods. During this integration process, the accelerometer signal will be monitored using a two-stage integration process. The major advantage of GBA in MEMS is that noise level will be reduced with a high extension of bandwidth. In addition, data will be normalized during the linear transformation state even at high acceleration values and thus minimum and maximum variations can be given as follows:

$$\rho = \frac{\text{norm}_{acc} - \text{norm}_{\min}}{\text{norm}_{\max} - \text{norm}_{\min}}. \tag{8}$$

Here, norm_{acc} indicates normalization of acceleration values $\text{norm}_{\min}$ and $\text{norm}_{\max}$ represents boundaries of normalization values.

From Equation (8), only slow accelerometer values can be normalized. But in critical cases, Equation (8) cannot extend support at varying time periods. Thus, normalization errors can be minimized using Equation (9) as follows:

$$RMS_i = \sum_{i=1}^{n} \sqrt{\frac{\delta_{\text{observed}} - \delta_{\text{reference}}}{\delta_{\text{in}}}}. \tag{9}$$

Equation (9) specifies that the difference between reference and observed values will be taken into account for the normalization process in GBA and these values will be distributed inside the loop. Also, during GBA, adequate exploration information in different directions can be found using several optimization iterations with high measures in performance. Therefore, loss functions can be expressed in the mathematical form as follows:

$$L_i = \sum_{i=1}^{n} \sqrt{\frac{e_{\text{in}}}{N}}, \tag{10}$$

where e_{in} denotes error values of end systems and N indicates maximum iteration values.

Since GBA depends on the learning rate, a power rule can be applied by assuming both coefficients as zero. Thus, power rule equation can be expressed as follows:

$$\frac{d(p)}{d(t)} = LR_i \sum_{i=1}^{n} \sqrt{2 * e_{\text{in}}}, \tag{11}$$

where LR_i represents the learning rate of information in corresponding direction.

2.1. Step-by-Step Implementation

Step 1. Determine the forecast procedure using sine and cosine central angles for both the vertical and horizontal positions.

Step 2. Measure the weight of individual tire system using terrain representations with a multiplication factor.

Step 3. Normalize the values using Equation (8) by following change of representations.

Step 4. If change of representations are found, then stop the iteration loop, and if no changes are found, then normalize the system using Equation (9).

Step 5. Obtain the loss functions with slip angle indications. In case if loss functions are found, then go back to Step 4.

Step 6. If loss functions are not found, then the loop can be stopped and learning rate will be observed.

Step 7. Critical case study with rotation angles is done with reduction in error functions. At the final state, observe time-varying velocities and print the values.

3. Outcomes

The drive on the puncture tire axle is placed in the middle of the tire. Hence, it neglects the pressure that needs to be applied, to move the drive machine. The work applied to the drive machine by the vehicle is fully distributed by the axle to the drive machine wheels. Also, the work is defined as the force applied on the object multiplied by the distance traveled. Mathematically, it is represented as work (w) = force $(F) * $ distance (D). CATIA 3D experience software presents the prototype of the model of any product. Also, it provides the context of the products in real-time environment.

Figure 2 shows the image of the drive on the puncture tire, which was designed using CATIA 3D experience. The drive on the puncture wheel was designed using the part design sketcher. The drive on the puncture tire product has to be about 1000 kg car weight. Hence, the mild steel was added as a base material. Mild steel was a high-strength alloy with less weight. The drive on the puncture wheel is a simple device that consists of two circular wheels and an axle. The device is attached with electronic control system, which controls the stability of the device with respect to the speed of the vehicle. Figure 3 shows the CATIA 3D design and simulation of the drive on the puncture wheel in different views. The main advantages of this drive on the puncture tires were no requirement to change the flat tire by the side of the road and fitting on both front and rear tires. The drive on the puncture tire is capable of withstanding up to 2000 kg of weight. The drive on the puncture tire allows the vehicle to drive up to 30 km/h. The drive on the puncture tire reduces an accident that prevents driving risks, such as tire reduction and blowouts. The frame of the drive on the puncture tire is made up of mild steel. The mild steel is generally suitable for high strength-to-weight ratio.

The drive on a flat tire is specially designed and simulated to keep working for a short distance even after the tire is punctured. So if one gets a punctured tire on a cold, dark night, there is no need for an uncomfortable roadside tire change; you should be able to safely drive to home garage to get your tire changed. The drive on a flat tire also limits the risk of a potentially dangerous tire blowout. The drive on the flat tire is made with reinforced sidewalls. Normally, a car is supported by the air in your tires, and once we have a puncture, they collapse. Once the vehicle tire is punctured, it is not possible to drive on it forever. The materials used to fabricate the drive on the puncture tire are similar to conventional tire, so wear rates should be identical. Researchers around the world clearly describes the importance of tires, which plays an important role in the vehicle dynamics. Most importantly, tires are exposed to hectic conditions like severe temperature and continuous hitting of debris in tires in their life time.

The drive on flat tires protects the tires after they get punctured by lifting the tires from the ground state. The drive on the puncture tire does the mechanical action to move the vehicle for a short distance and protects the flat tire. Moreover, the drive on the flat tire device minimizes the work of flat tire. To further explore the mechanical actions, two scenarios are simulated with the established system model using a MATLAB simulator by designing a vehicle system using the same dimensions.

3.1. Scenario 1. In this scenario, the slip angle of tire is measured with respect to rotation time periods where data are observed continuously for five days. During this process, the step angles are increased slowly from 0 as the sudden change in angle measurement will rupture the tire. Therefore, due to slow varying period, the number of observations is also increased, thus providing precise values even under complex scenarios. As a target point with a MEMS accelerometer, the speed of the vehicle is increased to a certain point before rotation and it is observed that changes are reported without any loss of functionality. But, the problem has been observed with increasing speed with rotation angles and it is safe to drive at 30–40 kph in case of spinning wheels. The curve points are shaped to provide high safety in both latitude and longitude positions using arctan values. The simulated rotation angle and speed are illustrated in Figure 4.
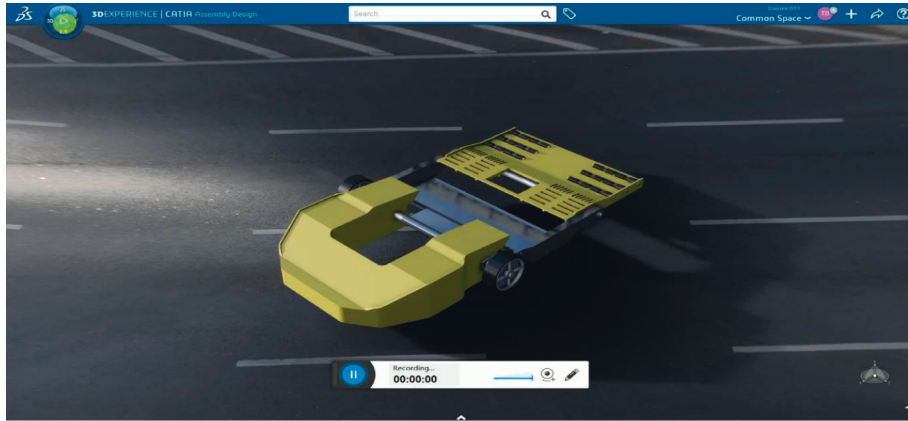
FIGURE 2: CATIA 3D experience design of the drive on the puncture tire.

(a)

(b)

(c)

(d)

FIGURE 3: CATIA 3D design and simulation of the drive on the puncture wheel in different views.

It can be observed from Figure 4 that the time period is changed from 6 AM to 10 PM and for the remaining time periods, the applied speed and change angles will be the same; thus, it is neglected from system observations. In this comparison measurement, two plots are divided as speed and rotation angles are measured in the primary case whereas rotation and slip angles will be restrained as a secondary parameter. In critical conditions, it is better to observe values with a rotation of 360° by supplying a high accelerometer speed which is equal to 35 km/h. After a certain period of time, it is found that slip angles are much less as the control technique with the MEMS system is activated as compared to normal systems. Even at critical conditions, only 23 degrees of slip is measured; this proves that the designed system model will function effectively at all circumstances.

3.2. Scenario 2. The time period of measurement is one of the important constraints as the speed of movement is increased to a maximum extent. Therefore, in this scenario, the time
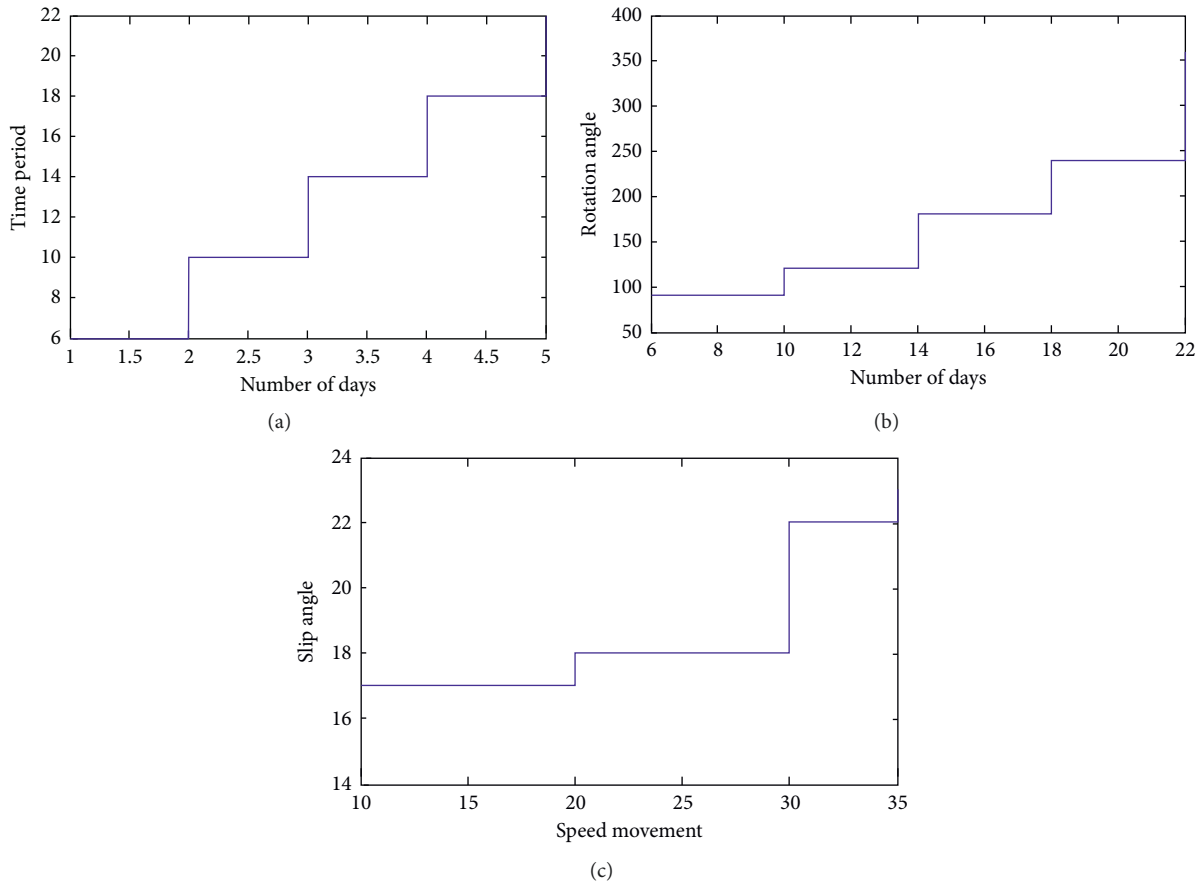
(a)

(b)

(c)

FIGURE 4: Measurement of the slip angle. (a) Time period. (b) Rotation angle. (c) Slip angle.
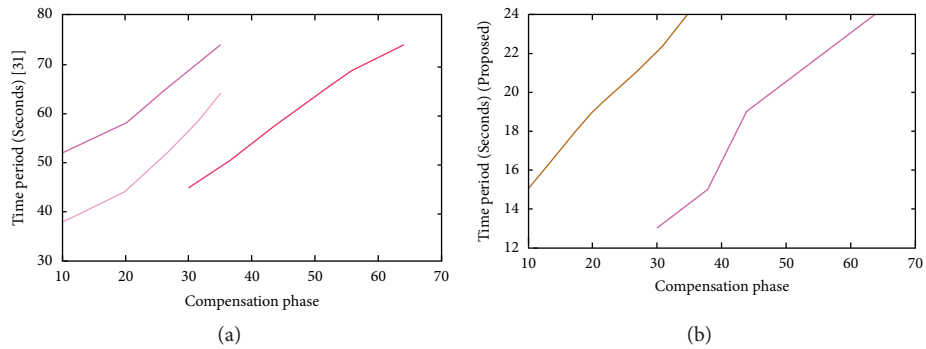

(a)

(b)

FIGURE 5: Time period. (a) Existing approach. (b) Proposed model.

period of calculation is measured with respect to the applied force. In case if the time of measurement is much higher than expected, a compensation phase will be created for the critical applied force. The abovementioned process is termed as secondary phase conditions which control the signals that are applied at the input side. However, with the application of the MEMS accelerometer, it is not possible to apply all data at the same time period for measurement, but as mentioned in scenario 1, a small step period can be provided at the initial phase. Thus, an initial starting period of $t = 0.5$ is automatically stored at the end systems. Figure 5 deliberates the time period of measurement using MEMS GBS.

From Figure 5, it can be perceived that speed of movement is reserved in the same that is present in scenario 1, whereas compensation phases are introduced with a moving accelerometer. This provides a great advantage for all moving systems as automatic speed adjustment can be processed at the transmitting phase. Thus, the proposed system period is reduced with addition to the compensation phase, whereas in the existing system [31] even with compensation time, measurement is much higher. This can be proved for the critical system when the speed of the vehicle is 35 km/h, where a compensation value of 64 is added, thus leading to reduced time which is equal to 24 seconds. But

with the same specification, the existing method can measure the values and reports them at a maximum time of 74 seconds. This measurement will increase if the system becomes more critical and highly occupied. Also, if possible, with using nanomaterials with high strength to less weight ratio [33–38], the efficiency of the product will increase.

4. Conclusions

The run-on flat tire is an important technology in the area of vehicle safety technology. Nowadays, traveling by a personal vehicle from one place to another has increased due to the increase in the global economy. The main problem that is faced while traveling is tire puncture. For this reason, a design has been developed by the CATIA 3D experience. The drive on a puncher tire device was designed using the software developed by the Dassault systems named CATIA 3D experience. Aluminum alloy was chosen as the base material to design and simulate this product. This device is very useful while traveling long distances in case if any puncher occurs. The sensors were attached to the product to receive the signal from the vehicle, so that vehicle will run smoothly for a short distance. Drive on a puncher tire will be suitable for both two- and four-wheeler vehicles and also useful for all the areas like the village, town panchayats, and cities. If the tire is punctured, we cannot drive the vehicle; hence, a skating device is fixed at the tire's bottom, which is used to move the vehicle. The proposal will be beneficial for the huge number of people who own two and four wheelers. This design and simulation will address the problem of the two- and four-wheeler owners traveling long distances.

Data Availability

The data used to support the findings of this study are available from the corresponding author upon request.

Conflicts of Interest

The authors declare that they have no conflicts of interest.

Acknowledgments

References

[1] L. Zang, Y. Cai, B. Wang, R. Yin, F. Lin, and P. Hang, "Optimization design of heat dissipation structure of inserts supporting run-flat tire," *Proceedings of the Institution of Mechanical Engineers - Part D: Journal of Automobile Engineering*, vol. 233, no. 14, pp. 3746–3757, 2019.

[2] W. L. Willard Jr, *Run-flat Tire with Three Carcass Layers*, Google Patents, Mountain View, 1995.

[3] E. G. Markow, *Run-flat Tire Incorporating Tape-Wrapped Helical Coil Band and Method of Forming*, Google Patents, Mountain View, 1987.

[4] E. G. Markow and M. A. Kopsco, *Run-flat Tire and Method of Making Same*, Google Patents, Mountain View, 1984.

[5] H. J. Mirtain and A. M. Devienne, *Run-flat Tire and Hub Therefor*, Google Patents, Mountain View, 1977.

[6] R. S. Cataldo, *Run-flat Tire Having Integral Internal Support Means*, Google Patents, Mountain View, 1979.

[7] I. Osada and S. Sano, *Run-flat Support and Tire Assembly*, Google Patents, Mountain View, 1982.

[8] R. S. Cataldo, *Run-flat Tire and Wheel Arrangement with Inverted Bead Interlock*, Google Patents, Mountain View, 1979.

[9] P. S. Hammond, T. R. Oare, G. E. Tubb, W. M. Buckler, and R. A. Losey, *Run-flat Tire with Wet Handling Design*, Google Patents, Mountain View, 1997.

[10] A. Deck and C. Lefaucheur, *Safety Tire with Sidewall Support Members Having Two Parts with Different Flexibilities*, Google Patents, Mountain View, 1981.

[11] E. Nakaski and Y. Igarashi, *Run-flat Tire and Rim Assembly for ATV*, Google Patents, Mountain View, 1990.

[12] J. R. Cho, J. H. Lee, K. M. Jeong, and K. W. Kim, "Optimum design of run-flat tire insert rubber by genetic algorithm," *Finite Elements in Analysis and Design*, vol. 52, pp. 60–70, 2012.

[13] M. Davis, *It's Only a Flat Tire in the Rain*, Penguin, Antarctica, 2002.

[14] J. S. Baker and L. B. Fricke, *The Traffic-Accident Investigation Manual: At-Scene Investigation and Technical Follow-Up*, Northwestern University Traffic Institute Evanston, Evanston, 1986.

[15] C. Y. Warner, G. C. Smith, M. B. James, and G. J. Germane, *Friction Applications in Accident Reconstruction*, SAE Technical Paper, Edinburgh, UK, 1983.

[16] E. Z. Klein and T. L. Black, "Anatomy of accidents following tire disablements," *SAE Technical Paper 0148-7191*, vol. 21, 1999.

[17] W. M. Hopkins, S. P. Landers, and S. F. Roth, *Tire Initiated Vehicle Control System*, Google Patents, Mountain View, 2002.

[18] S. D. Ko, *Internal Tire Support Wheel*, Google Patents, Mountain View, 1991.

[19] A. Yoshida and M. Kan, *Pneumatic Safety Tire*, Google Patents, Mountain View, 1982.

[20] H. Noma and S. Saitou, *Radial Tire Which Runs Safe after a Loss of Tire Pressure*, Google Patents, Mountain View, 1992.

[21] A. Segoni, *Accident Signalling Device*, Google Patents, Mountain View, 1957.

[22] S. Venkatesan, B. Visvalingam, G. Mannathusamy, and A. Viswabaskaran Viswanathan, "Gourav Rao, Mechanical and Tribological Properties of Self-Lubricating Al 6061 Hybrid Nano Metal Matrix Composites Reinforced by nSiC and MWCNTs," *Surfaces & Interfaces Elsevier*, vol. 21, 2020.

[23] J. Jaehyung, A. Balajee, D. S. Joshua, and P. Joseph, "Design of cellular shear bands of a non-pneumatic tire-investigation of contact pressure," *SAE Int J Passeng Cars-Mech Syst*, vol. 3, pp. 598–606, 2010.

[24] T. B. Rhyne and S. M. Cron, "Development of a non-pneumatic wheel," *Tire Science and Technology*, vol. 34, p. 150, 2006.

[25] X. Jin, C. Hou, and X. Fan, "On the static and dynamic behaviors of non-pneumatic tires with honeycomb spokes," *J Compos Struct*, vol. 187, pp. 27–35, 2018.

[26] I. G. Jang, Y. H. Sung, E. J. Yoo, and B. M. Kwak, "Pattern design of a non-pneumatic tyre for stiffness using topology optimization," *Engineering Optimization*, vol. 44, pp. 119–131, 2012.

[27] L. Zang, Y. Cai, B. Wang, R. Yin, F. Lin, and P. Hang, "Running mechanism of run-flat tire with inserts in zero pressure," *Journal of Tsinghua University*, vol. 54, pp. 871–876, 2014.

[28] X. Yang, "Virtual design and performance analysis of run flat inserts," *PhD Thesis*, Jilin University, Changchun, China, 2007.

[29] X. Dongpin and D. Guang, *Tyre Burst Detecting and Anti-deviation System and Method*, United States Patent Application Publication, Mountain View, 2012.

[30] I. Kuric, J. Klarák, M. Sága, M. Císar, A. Hajdučík, and D. Wiecek, "Analysis of the possibilities of tire-defect inspection based on unsupervised learning and deep learning," *Sensors*, vol. 25, p. 21, 2021.

[31] N. Xu, H. Askari, Y. Huang, J. Zhou, and A. Khajepour, "Tire force estimation in intelligent tires using machine learning," *IEEE Transactions on Intelligent Transportation Systems*, vol. 23, pp. 1–10, 2020.

[32] D. Rybarczyk, "Application of the mems accelerometer as the position sensor in linear electrohydraulic drive," *Sensors*, vol. 21, pp. 1–15, 2021.